PNAS RESEARCH ARTICLE | BIOCHEMISTRY

Natural photoredox catalysts promote light-driven lytic polysaccharide monooxygenase reactions and enzymatic turnover of biomass

Eirik G. Kommedal[a], Fredrikke Sæther[a], Thomas Hahn[b], and Vincent G. H. Eijsink[a,1]

Edited by Donald Ort, University of Illinois at Urbana Champaign, Urbana, IL; received March 16, 2022; accepted July 11, 2022

Lytic polysaccharide monooxygenases (LPMOs) catalyze oxidative cleavage of crystalline polysaccharides such as cellulose and chitin and are important for biomass conversion in the biosphere as well as in biorefineries. The target polysaccharides of LPMOs naturally occur in copolymeric structures such as plant cell walls and insect cuticles that are rich in phenolic compounds, which contribute rigidity and stiffness to these materials. Since these phenolics may be photoactive and since LPMO action depends on reducing equivalents, we hypothesized that LPMOs may enable light-driven biomass conversion. Here, we show that redox compounds naturally present in shed insect exoskeletons enable harvesting of light energy to drive LPMO reactions and thus biomass conversion. The primary underlying mechanism is that irradiation of exoskeletons with visible light leads to the generation of H_2O_2, which fuels LPMO peroxygenase reactions. Experiments with a cellulose model substrate show that the impact of light depends on both light and exoskeleton dosage and that light-driven LPMO activity is inhibited by a competing H_2O_2-consuming enzyme. Degradation experiments with the chitin-rich exoskeletons themselves show that solubilization of chitin by a chitin-active LPMO is promoted by light. The fact that LPMO reactions, and likely reactions catalyzed by other biomass-converting redox enzymes, are fueled by light-driven abiotic reactions in nature provides an enzyme-based explanation for the known impact of visible light on biomass conversion.

lytic polysaccharide monooxygenases | photobiocatalysis | biomass conversion | insect exuviae | catecholamines

Significance

Microbial decomposition of organic litter is faster above ground than below ground, and this effect has been attributed to sunlight-driven modification of aromatic constituents, leading to increased susceptibility of polysaccharides to enzymatic degradation. We show that such light effects may in fact be due to photobiocatalytic reactions involving polysaccharide-degrading lytic polysaccharide monooxygenases (LPMOs) and redox-active aromatic constituents of the biomass substrates such as catecholamines in insect exoskeletons and lignin in plant material. By using insect exoskeletons, we show that light promotes abiotic generation of H_2O_2, which fuels LPMO peroxygenase reactions. Thus, we provide an enzymatic explanation for why light promotes biomass conversion and generate insight into the enzymology of LPMOs, which are widespread throughout nature.

Transitioning from non-sustainable fossil feedstocks to sustainable renewable feedstocks for chemicals and energy demands efficient processes for converting renewable resources into chemicals and energy (1). Plant and insect biomass represent vast reservoirs of crystalline polysaccharides, such as cellulose and chitin, respectively, but the complex nature of plant cell walls and insect exoskeletons complicates the extraction and valorization of these carbohydrates. Cellulose-degrading and chitin-degrading microorganisms have solved this challenge by developing advanced enzymatic tools for biomass processing, with a major impact on the global carbon cycle.

A key and relatively recently discovered group of enzymes used for biomass conversion contain the lytic polysaccharide monooxygenases (LPMOs) (2–4), which are monocopper enzymes (5, 6) that oxidatively cleave glycosidic bonds in chitin (4) and cellulose (5–7). LPMOs are widespread in terrestrial ecosystems and are classified in the auxiliary activity (AA) families 9–11 and 13–17 of the Carbohydrate-Active enZYmes (CAZy) Database (8). At the time of discovery, LPMOs were considered to be monooxygenases, but recent work has shown that H_2O_2 is a kinetically relevant cosubstrate that allows fast peroxygenase reactions (9–17). LPMOs are ubiquitous enzymes that play an important role in fungal and bacterial biomass conversion by introducing chain breaks in the crystalline surfaces of chitin or cellulose. By doing so, LPMOs enhance the depolymerization activity of glycoside hydrolases in nature as well as in commercial enzyme mixtures used at industrial scale. Importantly, the discovery of LPMOs has revealed that redox processes are important for polysaccharide conversion in the biosphere, as suggested some 50 years ago (18), which provided new insights and raised new questions regarding the interplay between the many components of natural biomass-converting enzyme systems (19).

LPMO catalysis requires two reducing equivalents per catalytic cycle, which, depending on the catalytic mechanism being considered, are delivered to the copper site (monooxygenase reaction) or used to convert O_2 to H_2O_2 to enable a peroxygenase reaction (20) (Fig. 1). It is currently being debated whether apparent monooxygenase reactions, which typically entail incubating the LPMO with substrate and a reductant

Author contributions: E.G.K., T.H., and V.G.H.E. designed research; E.G.K. and F.S. performed research; E.G.K. and T.H. contributed new reagents/analytic tools; E.G.K., F.S., and V.G.H.E. analyzed data; and E.G.K., F.S., T.H., and V.G.H.E. wrote the paper.

The authors declare no competing interest.

This article is a PNAS Direct Submission.

[1]To whom correspondence may be addressed. Email: vincent.eijsink@nmbu.no.

This article contains supporting information online at http://www.pnas.org/lookup/suppl/doi:10.1073/pnas.2204510119/-/DCSupplemental.

Published August 15, 2022.

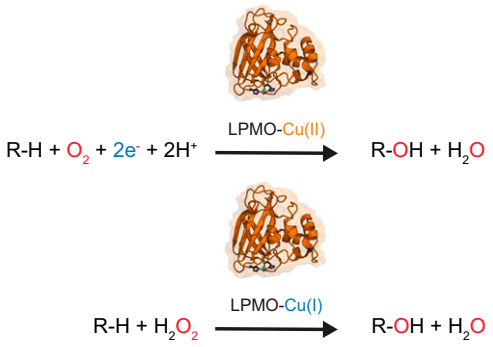

Fig. 1. Possible reaction schemes for LPMOs. In the upper monooxygenase reaction, every catalytic cycle requires channeling of two electrons and two protons to the catalytic center. In the lower peroxygenase reaction, a once-reduced (primed) LPMO can catalyze multiple reactions using H_2O_2 as cosubstrate without any further delivery of protons or electrons (9, 12, 13). Occasionally, LPMOs may become oxidized through off-pathway reactions (14, 21), and re-reduction is then required to regain catalytic competence.

under aerobic conditions, are true monooxygenase reactions or whether these are peroxygenase reactions that are limited by *in situ* generation of H_2O_2. While the apparent monooxygenase reaction entails stoichiometric consumption of reductant, it has been shown that a once-reduced LPMO can catalyze multiple peroxygenase reactions if it is supplied with H_2O_2. The average number of peroxygenase reactions catalyzed by a reduced LPMO has been reported to be on the order of 20 (13, 14). H_2O_2-driven LPMO catalysis is a double-edged sword, because too much H_2O_2 leads to inactivation of the LPMO through non-productive turnover accompanied by oxidative damage to the enzyme (9, 21), while too low access to H_2O_2 leads to low enzyme activity.

Insect cuticles and plant cell walls, which are major components of organic litter in nature (22), are complex and rigid copolymeric structures, which next to chitin and cellulose, respectively, contain light-sensitive aromatic compounds with quinone/hydroquinone redox-active moieties. The impact of LPMOs on polysaccharide conversion and the notion that these enzymes act on redox-active copolymeric substrates, raise the questions of whether and how light affects LPMO activity and thus biomass turnover. Light is an abundant and cheap source of energy that, in the presence of a photoredox catalyst and O_2, can fuel H_2O_2-dependent enzyme reactions (23–25). It has been demonstrated that lignin, a major aromatic component of plant cell walls, can act as a photocatalyst for solar-powered H_2O_2-dependent enzyme reactions (26). Photobiocatalytic LPMO reactions were first demonstrated in 2016 for a fungal LPMO acting on amorphous phosphoric acid swollen cellulose (PASC) by combining a photosynthetic pigment, chlorophyllin, and a reductant, ascorbic acid (AscA) (27). Later the same year, it was shown that vanadium-doped titanium dioxide (V-TiO_2) allowed light-driven activity of a bacterial LPMO from *Streptomyces coelicolor* (*Sc*AA10C) on crystalline cellulose (Avicel) (28). Both studies discussed the underlying mechanisms for photobiocatalytic LPMO activity but did not consider peroxygenase activity. Later, it was shown that light-induced formation of H_2O_2 from O_2 was the main driver of these photobiocatalytic LPMO reactions (24).

Shed chitin-rich exoskeletons resulting from insect moulting, collectively referred to as pupal exuviae (PE), consist of a complex matrix of chitin, proteins, and potentially photosensitive phenolic compounds, in particular catecholamines (29). The latter are incorporated during sclerotization to provide stiffness, hardness, and resistance toward the environment and are responsible for the dark color of the exuviae (30). Considering their photosensitivity, we hypothesized that the catecholamines present in PE may act as a photoredox catalyst for *in situ* generation of H_2O_2, which could be used to fuel LPMO-catalyzed turnover of insect biomass in nature.

To test this hypothesis, we first carried out a detailed study of the degradation of a model cellulose substrate by a well-studied LPMO from the soil actinomycete *S. coelicolor* (*Sc*AA10C), using light-exposed PE for fueling the reaction. We showed that exposure to light has a large effect on LPMO activity that correlates with light-fueled generation of H_2O_2. Subsequent studies of the depolymerization of chitin in the PE themselves with a chitin-active LPMO (*Sm*AA10A) showed that exposure to visible light has a similar effect on this LPMO and promotes turnover of insect biomass. Thus, our study provides a possible mechanistic framework for the effect of light on biomass turnover in the biosphere.

Results

Proof of Concept: Fueling LPMO Reactions with Insect Exoskeletons (PE) as a Photocatalyst. To assess the ability of insect biomass to fuel LPMO reactions, we used a well-studied C1-oxidizing cellulose-active LPMO from *S. coelicolor* (*Sc*AA10C; also known as CelS2) and Avicel (i.e., crystalline cellulose). A reaction in the dark with gallic acid, a commonly used reductant in standard LPMO reactions, was included as a reference reaction. The PE contain 20% (wt/wt) chitin and 12.6% (wt/wt) phenolic compounds (31). Washing the PE removed soluble compounds absorbing in the 240 nm to 800 nm range (*SI Appendix*, Fig. S1) and reduced the total reducing capacity by 72% as measured by the Folin-Ciocalteu assay (32) using gallic acid as a standard (*SI Appendix*, Fig. S2).

Progress curves for Avicel conversion (Fig. 2) showed linear product formation over 6 h for all reactions, except for the reactions lacking PE or gallic acid, which did not show any LPMO activity, and the light-exposed reaction with non-washed PE, which showed a high initial LPMO rate that started decreasing after ~2 h. The reactions with washed or non-washed PE in the dark produced identical very low product levels during the 6-h incubation period, and apparent reaction rates were more than one order of magnitude lower compared with the reactions exposed to visible light (Fig. 2). Reactions in which the LPMO was replaced by an equal concentration of $CuSO_4$ did not show formation of oxidized products (*SI Appendix*, Fig. S3).

Compared with the reference reaction with 1 mM gallic acid, the reaction with light-exposed washed PE was about two times faster and produced two times more product over 6 h, despite the fact that the concentration of gallic acid equivalents in the reaction with exuviae equaled only some 0.2 mM (*SI Appendix*, Fig. S2). The large impact of light is further evidenced by the observation that the reactions with PE in the dark were an order of magnitude slower than the reaction with gallic acid for both the washed (0.2 mM gallic acid equivalents) and the non-washed (0.6 mM gallic acid equivalents) materials (Fig. 2).

While the redox state of the catecholamines that are incorporated into the cuticular matrix is not known (33), it is likely that their quinone/hydroquinone moieties are photoredox active in aqueous solutions, as exemplified by the role of plastoquinone in photosynthetic water splitting in photosystem II (34). There are other examples: under aerobic conditions, ultraviolet (UV) light will convert hydroquinone to benzoquinone,

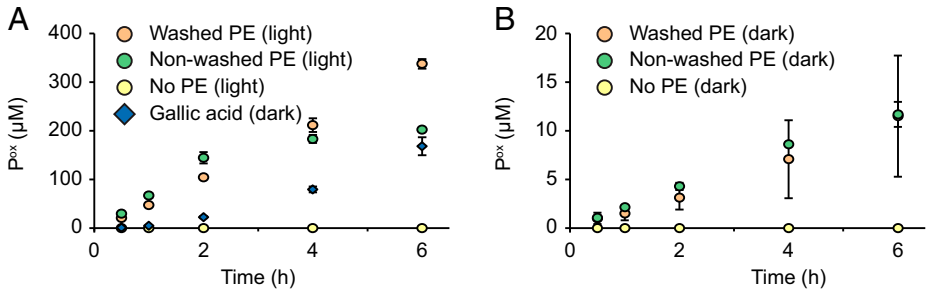

Fig. 2. *Sc*AA10C-catalyzed cellulose oxidation fueled by photocatalytic insect exoskeletons. The graphs show time courses for the formation of solubilized oxidized products by *Sc*AA10C (0.5 μM) in reactions with Avicel (10 $g.L^{-1}$) in sodium phosphate buffer (50 mM, pH 6.0) at 40 °C under magnetic stirring (*A*) with and (*B*) without irradiation by visible light (note the different scaling of the Y-axes). The reactions contained washed or non-washed PE (5 $g.L^{-1}$) or gallic acid (1 mM). Based on a determination of total reducing equivalents (*SI Appendix*, Fig. S2), 5 $g.L^{-1}$ corresponds to ∼0.2 mM gallic acid equivalents for the washed material and 0.6 mM gallic acid equivalents for the nonwashed material. Reactions were incubated with magnetic stirring in the dark or exposed to white light (I = 10% I_{max}; ∼16.8 $W.cm^{-2}$). Before the product was quantified, solubilized oxidized cello-oligosaccharides were converted to a mixture of cellobionic acid and cellotrionic acid by incubation with *Tf*Cel6A at room temperature overnight. The data points represent the mean of three independent experiments and error bars show ± SD. The high SDs in *B* are due to product levels being very low.

hydroxybenzoquinone, and H_2O_2 (35), whereas irradiation using 416 nm at pH 6.0 yields benzoquinone in a reactive triplet excited state, which leads to the production the semiquinone radicals $Q^{-\bullet}$ and $QH^{\bullet}$ (36). Regardless of light intensity and wavelength, the primary photochemical process for benzoquinone is reduction (37). Upon exposure to light, the catecholamines in insect cuticles may undergo reactions similar to those known for other quinones and hydroquinones to generate both the reducing conditions needed for the LPMO to become catalytically active and the H_2O_2 needed to oxidize the polysaccharide substrate. The results depicted in Fig. 2 show that indeed this is the case.

It is worth noting that the reaction with unwashed exuviae in the light shows a progress curve that is typical for LPMO reactions that contain too much H_2O_2 (16, 24, 38): the (too) high availability of the cosubstrate leads to a high catalytic rate but also to rapid enzyme inactivation. This suggests that washing removes redox-active compounds that contribute to light-induced production of H_2O_2. Indeed, during the course of this work, we noted that chitin-free watery extracts of the PE obtained by washing or during the demineralization and deproteination steps that are carried out when purifying chitin from the exuviae (31) could drive LPMO reactions when irradiated with light (*SI Appendix*, Fig. S4).

To verify whether the low activity in reactions with exuviae in the dark was due to lack of H_2O_2 generation, a control experiment was performed with 5 g/L washed PE in which 50 μM H_2O_2 was added after 0, 30, and 60 min, and the reaction was sampled at 30, 60, and 90 min (before the addition of H_2O_2). It is well known from earlier work with *Sc*AA10C that addition of this amount of H_2O_2 yields a fast reaction, provided that the reaction contains sufficient reducing power to produce the LPMO in its catalytically competent reduced state (9). *SI Appendix*, Fig. S5 shows that the dark reaction with exuviae was not boosted by the addition of H_2O_2, suggesting that reduction of both LPMO and H_2O_2 availability were limiting LPMO activity in the dark, which is not surprising considering that the reduction potential of a catecholamine model compound does not favor reduction of *Sc*AA10C (39).

Characterization of the Photobiocatalytic System. Encouraged by the successful proof-of-concept experiments, we investigated the influence of the PE concentration, light intensity, and substrate concentration on LPMO activity (Fig. 3). We also monitored H_2O_2 accumulation to unravel possible correlations between LPMO activity and H_2O_2 production.

Increasing the PE concentration from 1.25 to 20 g/L led to a threefold increase in the apparent rate for the LPMO reaction (Fig. 3 *A* and *C*), from 0.5 $\mu M \cdot min^{-1}$ at 1.25 g/L to 1.5 $\mu M \cdot min^{-1}$ at 20 g/L (Fig. 3*C*), as well as a near sixfold increase in the apparent rate of H_2O_2 generation, from 0.12 $\mu M \cdot min^{-1}$ at 1.25 g/L to 0.75 $\mu M \cdot min^{-1}$ at 20 g/L (Fig. 3 *B* and *C*). Conducting reactions with increasing light intensities showed a clear dose-response effect and resulted in an increase of two orders of magnitude in the apparent rate of the LPMO reaction, from 0.02 $\mu M \cdot min^{-1}$ in the dark to 2.2 $\mu M \cdot min^{-1}$ for the highest light intensity applied (Fig. 3 *D* and *F*). H_2O_2 production also increased at higher light intensities (Fig. 3*E*), and the apparent rate of H_2O_2 formation showed a linear correlation with the light intensity (Fig. 3*F*). Cellulose particles present in the reaction vessel reduce light transmittance (38) and, indeed, higher Avicel concentrations led to lower LPMO activity (Fig. 3*G*) and lower H_2O_2 production (Fig. 3*H*). It is noteworthy that the reaction in the absence of Avicel produced most H_2O_2. Taken together, these results show that the combination of PE and light provides a tunable system for driving LPMO reactions and that LPMO activity is correlated with the ability of the system to produce H_2O_2.

The reactions with LPMO generally showed higher product formation than what can be accounted for by H_2O_2 accumulation in identical reactions in the absence of LPMO (Fig. 3). The H_2O_2 concentration measured in the LPMO-free reactions is the net result of formation and decomposition reactions that will be affected by both redox-active components in PE and by light. It has been shown that, in the presence of substrate, reduced LPMOs have high affinity for H_2O_2 [K_m values in the low micromolar range (15, 16, 21)]. Thus, it is conceivable that in the reaction with LPMO, H_2O_2 consumption in productive reactions with the enzyme outcompetes abiotic decomposition, which could help explain the product levels. Furthermore, reduction of the LPMO by light-exposed PE may speed up H_2O_2 production in two ways: (1) the resulting modification of the PE may yield compounds that more readily catalyze abiotic H_2O_2 production, and (2) the reduced LPMO may catalyze oxidase reactions yielding H_2O_2 (40).

Considering the observations indicating that access to H_2O_2 was limiting the reactions displayed in Fig. 3 and the possible involvement of the LPMO itself in H_2O_2 production, we then assessed whether the amount of LPMO could be limiting the standard reaction with Avicel (10 $g.L^{-1}$) and PE (5 $g.L^{-1}$). While the reaction with lowest LPMO concentration (100 nM) showed diminished product formation and cessation of the

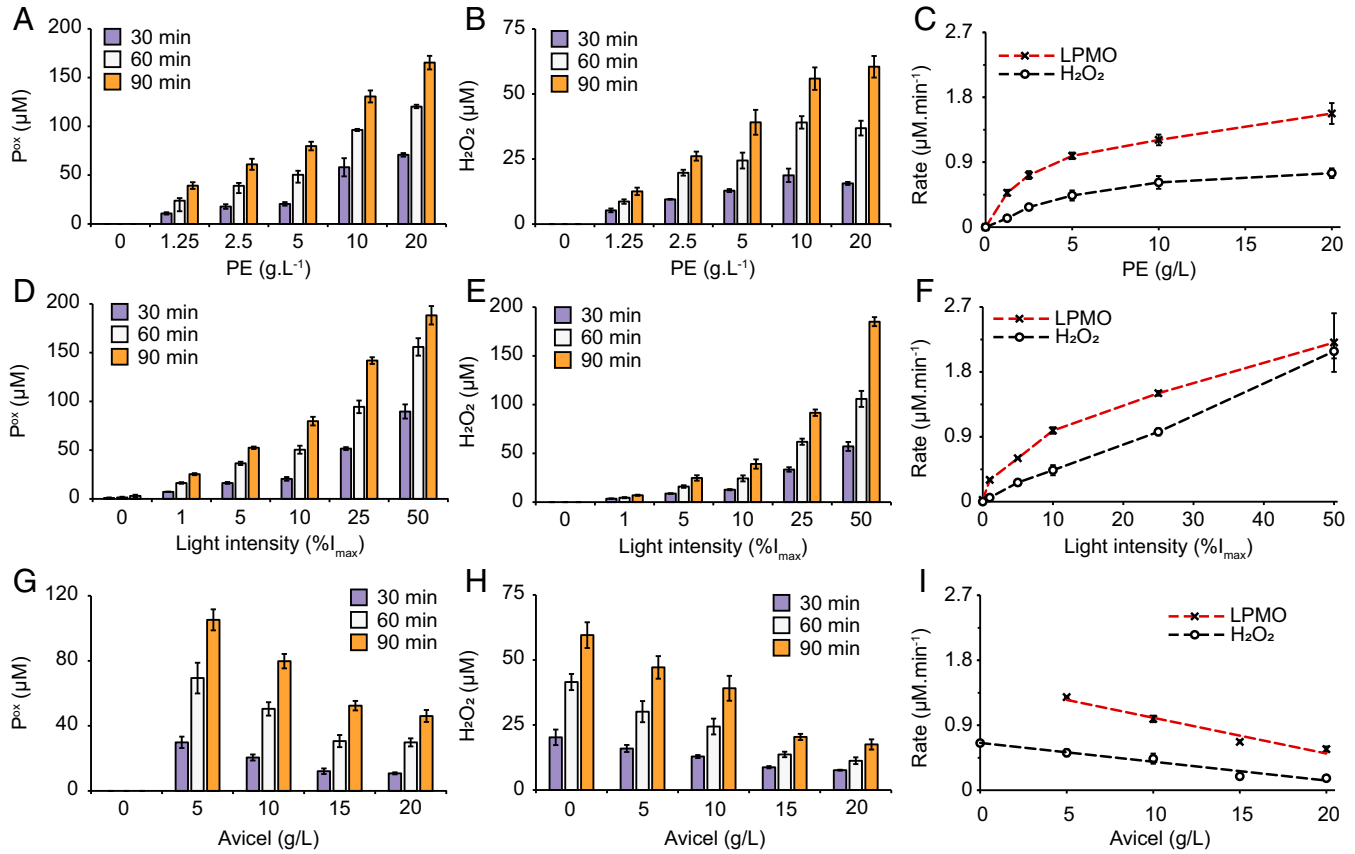

Fig. 3. Influence of PE loading, light intensity, and cellulose concentration on LPMO activity and H_2O_2 production. The graphs show time courses for the formation of solubilized oxidized products in LPMO (*Sc*AA10C, 0.5 µM) reactions with Avicel and exposed to light at (*A*) varying PE concentrations (10 $g.L^{-1}$ Avicel; I = 10% I_{max}; ~16.8 $W.cm^{-2}$), (*D*) light intensities (5 $g.L^{-1}$ PE; 10 $g.L^{-1}$ Avicel), and (*G*) Avicel concentrations (5 $g.L^{-1}$ PE; I = 10% I_{max}; ~16.8 $W.cm^{-2}$). (*B*, *E*, and *H*) H_2O_2 accumulation in equivalent reactions lacking the LPMO. The approximate rates obtained for LPMO activity and H_2O_2 accumulation were derived from the three shown time points for all reactions except the LPMO reaction with the highest light intensity (i.e., I = 50% I_{max}), for which only the first two time points were used. All regression analyses displayed an $R^2 > 0.98$. (*C*, *F*, and *I*) The approximate rates for LPMO activity and H_2O_2 accumulation are plotted against the variable parameter. Before product quantification, solubilized cello-oligosaccharides were converted to a mixture of cellobionic acid and cellotrionic acid by overnight treatment with *Tf*Cel6A at room temperature. The data points represent the mean of three independent experiments and error bars show ± SD. (*D* and *F*) Note that for the dark reaction, the final time point was 120 min and not 90 min, and that this is the same reaction as the reaction shown in Fig. 2.

reaction after about 1 h, product formation in the reactions containing 250 to 2,500 nM LPMO was linear over the 3-h incubation period and essentially independent of the LPMO concentration (Fig. 4 *A* and *B*). Thus, the LPMO concentration does not seem to be a limiting factor in the standard reaction conditions used in this study, further strengthening the idea that the light-driven formation of H_2O_2 determines LPMO activity.

To further demonstrate that it is the H_2O_2 generated from PE irradiated by visible light that drives the LPMO reaction, experiments were conducted with non-washed PE and increasing amounts of horseradish peroxidase (HRP). Here, nonwashed PE were used because the soluble phenolic compounds provide substrates for the peroxidase. The addition of increasing amounts of HRP resulted in increasing inhibition of the LPMO reaction (Fig. 4*C*). Approximately 11.4 nM HRP was required to achieve 50% inhibition of LPMO activity, and plotting the LPMO catalytic rates against the HRP concentration gave a reversed hyperbolic curve showing more than 95% inhibition of LPMO activity with 720 nM HRP (Fig. 4*D*). These experiments confirm the notion, derived from the above experiments, that H_2O_2 formation by irradiated PE is what drives the LPMO reaction.

Previous light-driven reactions with *Sc*AA10C have been performed using either chlorophyllin or V-TiO_2 as photocatalysts (24). In the case of reactions with chlorophyllin, $O_2^{\bullet-}$ production was demonstrated by showing that superoxide dismutase (SOD), which converts $O_2^{\bullet-}$ to H_2O_2, boosts LPMO activity (24). Later studies have since confirmed the production of $O_2^{\bullet-}$ by chlorophyllin (41). Conversely, such a boosting effect of SOD was not observed for LPMO reactions with V-TiO_2, leading to the conclusion that $O_2^{\bullet-}$ is likely not generated in this latter reaction system (24). Addition of SOD to a standard reaction with PE (5 $g.L^{-1}$), Avicel (10 $g.L^{-1}$) and *Sc*AA10C (0.5 µM) did not affect LPMO activity (Fig. 4*E*). A control reaction with boiled SOD showed identical product levels compared with the reactions with SOD, underpinning the notion that SOD does not affect the reaction (Fig. 4*E*). Additional experiments with increasing PE concentrations also did not reveal any effect of SOD (Fig. 4*F*).

The results depicted in Fig. 4 *E* and *F* indicate that superoxide does not play a role in this photocatalytic system and thus that H_2O_2 is produced directly by reduction of O_2 to H_2O_2 ($O_2 + 2H^+ + 2e^- \rightarrow H_2O_2$) or perhaps oxidation of H_2O to H_2O_2 ($2H_2O \rightarrow H_2O_2 + 2H^+ + 2e^-$), as has recently been shown for photoexcited lignin (26). Of note, for the chlorophyllin studies, superoxide was proposed to also act a reductant for the LPMOs. In the photoredox system that we studied, the LPMO is likely reduced by the photoredox-active compounds present in the PE, primarily upon exposure to light and possibly via formation of a semiquinone radical (36).

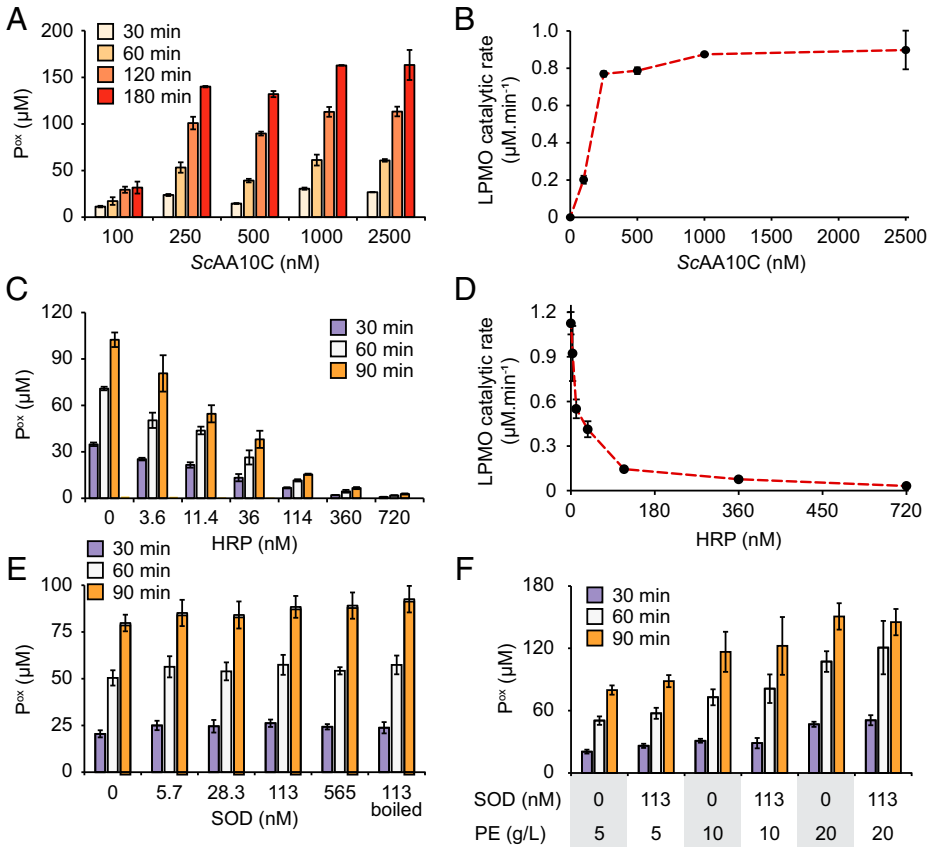

Fig. 4. Probing the role of reactive oxygen species in light-driven LPMO catalysis. The graphs show progress curves for the release of oxidized products from Avicel (10 g.L^{-1}) by *Sc*AA10C in the presence of varying amounts of (*A and B*) *Sc*AA10C, (*C and D*) HRP (with 0.5 µM LPMO), or (*E* and *F*) SOD (with 0.5 µM LPMO). All reactions were carried out in sodium phosphate buffer (50 mM, pH 6.0) containing 5 g.L^{-1} PE (unless indicated otherwise) at 40 °C under magnetic stirring and exposed to visible light (I = 10% I_{max}; ~16.8 W.cm^{-2}). (*F*) Data for reactions performed with varying concentrations of PE. The rates depicted in *B* and *D* were derived from the reactions in *A* and *C* using linear regression analysis (all time points, except for the reaction with 100 nM LPMO in *A* for which only the first three time points were used; $R^2 > 0.98$ in all cases). Before the product was quantified, solubilized cello-oligosaccharides were converted to a mixture of cellobionic acid and cellotrionic acid by treatment with *Tf*Cel6A at room temperature overnight. The reactions were performed as (*A*) duplicate and (*C*, *E*, and *F*) triplicate reactions, and error bars indicate ± SD. For the reactions in *A*, the difference was less than 10% between replicates for all time points except for the last time point with 2,500 nM *Sc*AA10C for which the difference was 16%. The data points for the standard reaction (i.e., 5 g.L^{-1} PE, 10 g.L^{-1} Avicel, and 0 nM SOD) in *E* and *F* are derived from the reaction with PE (5 g.L^{-1}) and Avicel (10 g.L^{-1}) that is displayed in Fig. 3 *A*, *D*, and *G*.

Light-Driven Solubilization of α-Chitin from *Hermetia illucens* PE. PE from black soldier flies contain ~20% chitin (31). Since PE exposed to visible light boosted the activity of *Sc*AA10C on cellulose, we investigated whether visible light could boost the ability of a chitin-active LPMO from *Serratia marcescens* (*Sm*AA10A; also known as CBP21) to solubilize the chitin present in the PE. For product quantification, soluble oxidized chito-oligomers were converted to a mixture of chitobionic acid and *N*-acetylglucosamine (GlcNAc) by treatment with a chitobiase (42). The light-exposed reaction with *Sm*AA10A led to rapid formation of chitobionic acid (Fig. 5*A*) with corresponding release of GlcNAc (Fig. 5*B*) during the first four h of the reaction, and product formation stopped after six h. The apparent minor increase in product levels between 6 h and 24 h is most likely due to liquid evaporation from the reaction vials. The reaction with *Sm*AA10A in the dark showed much slower but more linear formation of chitobionic acid (Fig. 5*A*) and corresponding release of GlcNAc (Fig. 5*B*).

Soluble oxidized products released by *Sm*AA10A are expected to contain between 4 and 10 monosaccharides (4). The product concentrations in Fig. 5 show that about five GlcNAc's were detected per chitobionic acid, indicating an average product length of seven monosaccharides, well in accordance with previous observations. Assuming a chitin content of 2 g/L, the product levels displayed in Fig. 5 indicate that ~7% of the chitin had been solubilized after 4 h in the light-exposed reaction. This fraction, 7%, is compatible with data previously reported for the action of *Sm*AA10A on β-chitin and likely represents the maximum that can be achieved by an LPMO acting in the absence of chitinases.

Discussion

It has been shown that irradiation of plant litter by sunlight, especially blue-green light, improves the biotic degradation of carbohydrates present in this material. This effect has been ascribed to photodegradation of lignin in the secondary plant cell walls, which would improve the accessibility of cell wall polysaccharides for enzymatic degradation (43–46). Studying chitin degradation, we show here that other mechanisms may be involved, and we provide a possible molecular explanation for the observation that light affects biomass turnover in nature. Chitin is abundantly present in terrestrial ecosystems, being a central structural component of many organisms, including insects, nematodes, and fungi. To our knowledge, nothing is known about the impact of light on chitin solubilization, and here we show that such impact can be large. Our findings suggest that light may not only contribute to the direct degradation of rigidifying structural components of plant cell walls and insect cuticles, as shown for lignins (43), but that the presence

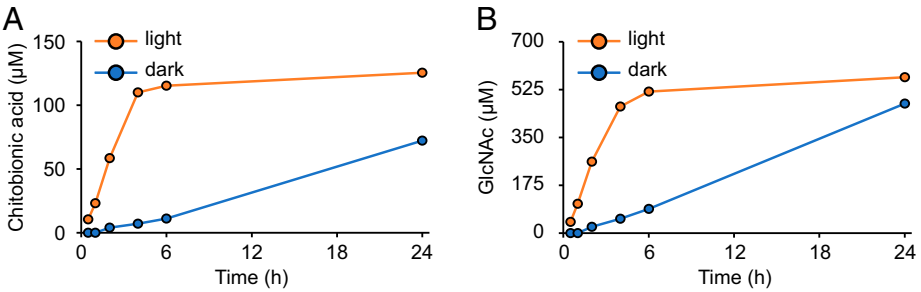

Fig. 5. Depolymerization of α-chitin from *H. illucens* PE by *Sm*AA10A. The graphs show time courses for the release of oxidized products from PE (10 $g.L^{-1}$, corresponding to a chitin concentration of ~2 $g.L^{-1}$ (31)) by *Sm*AA10A (0.5 μM) exposed to visible light (orange) or in the dark (blue). All reactions were carried out in sodium phosphate buffer (50 mM, pH 6.0) at 40 °C with magnetic stirring and exposed or not to visible light (I = 10% I_{max}; ~16.8 $W.cm^{-2}$). Before product quantification, solubilized chito-oligosaccharides were converted to chitobionic acid and *N*-acetylglucosamine (GlcNAc) by overnight incubation with *Sm*CHB (chitobiase, an N-acetylhexosaminidase) at room temperature (42), and both products are reported in *A* and *B*, respectively. The data points represent the mean of two independent experiments. Incubation of PE in the absence of enzymes did not yield detectable soluble products. Values obtained for the 24-h samples are overestimated due to liquid evaporation between 6 h and 24 h because the reactions are conducted in open glass vials.

of these photoredox-active components also plays a role in providing electrons and H_2O_2 to oxidative enzymes required for microbial biomass degradation.

It is known that aromatic compounds (e.g., derived from lignin) can fuel LPMO reactions even without irradiation (47) (Fig. 5). We show that the rate of such reactions is drastically enhanced upon irradiation and demonstrate high light-driven LPMO reactivity (7% chitin solubilization within a few hours; Fig. 5), but further studies are needed to unravel how critical LPMO action is for light-promoted biomass conversion in true ecosystems. Of note, natural biomass degrading aerobic enzyme systems tend to contain not only LPMOs but also other H_2O_2-dependent degradative enzymes, such as lignin peroxidases, which may benefit from light-promoted H_2O_2 production. Possible competition for H_2O_2 also needs to be considered; in this regard, it is worth noting that previous studies indicate that LPMOs have high affinity for H_2O_2 and catalytic efficiencies similar to those of common peroxidases and peroxygenases (15, 48). One interesting question for further research is whether the interplay among light, redox-active structural components, and enzymes such as LPMOs has affected the evolution of the materials and/or the enzyme systems that degrade them. Another interesting question is to what extent light provides a competitive advantage to those microbes that use LPMOs and other H_2O_2-dependent enzymes for biomass conversion.

Of note, sunlight is known to promote the degradation of organic matter and the formation of reactive oxygen species in aquatic ecosystems (49, 50). Thus, it is likely that the findings described here also apply to such ecosystems. In this respect, it is worth noting that a comparative study of bacterial genomes has shown that LPMOs are as common in aquatic chitinolytic bacteria as they are in terrestrial chitinolytic bacteria (51).

H_2O_2 is considered a green oxidant for agricultural, environmental, and industrial applications (52). Lignosulfonates and thin lignin films are known to act as homogeneous and heterogeneous photocatalysts, respectively, catalyzing the reduction of O_2 to H_2O_2 when exposed to a violet light-emitting diode (LED) source (λ_{max} = 400 nm) at the cost of lignin photodegradation (52). Similar to lignin, which for a long time was considered a waste product from the pulp industry (53), PE are currently considered as part of a waste stream from insect breeding and farming (31). We show here that this material, with its quinone/hydroquinone redox moieties (33), may be used for sustainable photocatalytic production of H_2O_2. Photons have been touted as a reagent for the twenty-first century (54), and using photons to generate H_2O_2 is an appealing green technology.

This study adds to the current debate on whether LPMOs are monooxygenases or peroxygenases by demonstrating correlations between light-driven LPMO activity and light-driven generation of H_2O_2 in the reaction system. Furthermore, we show that HRP inhibits light-driven LPMO catalysis, again suggesting the LPMO reaction depends on H_2O_2. The use of light and a photoredox catalyst may enable fine-tuning of the *in situ* generation of H_2O_2 and, consequently, polysaccharide oxidation by the LPMO. Such control is important since reduced LPMOs are prone to autocatalytic inactivation by surplus H_2O_2 (9, 55). Of note, the use of light to control the LPMO reactions in commercial bioreactors operating with substrates such as lignocellulose at high concentrations of dry matter will not be straightforward because light will not penetrate the reaction slurry.

The type of photoredox catalysts used in this study are abundantly present in the natural substrates of LPMOs and other biomass-degrading redox enzymes such as (H_2O_2-dependent) lignin peroxidases. Thus, our findings may have wide implications for biomass conversion in nature and should trigger further research in the area. Interestingly, these findings may relate to bulk biomass conversion and may also be relevant in other important biological processes. For example, it was recently shown that LPMO action promotes plant infection by the potato pathogen *Phytophthora infestans* (56); with the current results at hand, one may wonder whether the infection process could be light sensitive. If one assumes that light-driven H_2O_2 production is a significant contributor to the H_2O_2 pool in biomass degrading ecosystems, our current findings could even affect agronomic practices such as plowing. Plowing biomass into the soil will affect the activity of biomass-degrading peroxidases and peroxygenases not only by reducing access to O_2 but also by reducing access to the light that contributes to the reduction of O_2 to H_2O_2. No matter what the potential wider implications are, this study provides novel insights into the impact of light on biomass conversion in nature and the fascinating roles and catalytic abilities of LPMOs.

Materials and Methods

Materials. Unless otherwise stated, chemicals and enzymes were purchased from Sigma-Aldrich. The crystalline cellulose used was Avicel PH-101 (50-μm particles). PE from *H. illucens* were milled using a Retsch PM100 planetary ball mill with zirconium oxide vessels (500 mL) containing zirconium oxide balls (10 × 10 mm). Milled PE were sieved through a 0.85-mm stainless steel sieve (Retsch) and stored at 4 °C. A PE stock suspension of 50 g/L was prepared fresh each day, was washed four times by cycles of centrifugation (2 min, 15,000 × *g*), and was resuspended in sodium phosphate buffer (25 mM, pH 6.0) to remove soluble components, unless otherwise specified. The UV-visible light (UV-Vis) absorption spectrum for

the supernatant from each washing step was measured to monitor the removal of soluble components absorbing between 240 and 800 nm (*SI Appendix*, Fig. S1) using a UV-transparent 96-well microtiter plate in a Varioskan Lux plate reader (Thermo Fisher Scientific). Stock solutions of AmplexRed (Thermo Fisher Scientific) and gallic acid were prepared in dimethyl sulfoxide (DMSO) (10 and 100 mM, respectively), aliquoted, and stored at −20 °C in the dark. Gallic acid and AmplexRed aliquots were thawed in the dark for 10 min before use and were used only once.

Enzymes. Recombinant *Sc*AA10C (UniProt Q9RJY2) from *S. coelicolor* was produced and purified as previously described (7). *Sc*AA10C was copper saturated according to Loose et al (42), carefully desalted using a PD MidiTrap column [G-25, GE Healthcare (57)], and stored in sodium phosphate (25 mM, pH 6.0). The LPMO from *S. marcescens* (*Sm*AA10A; UniProt O83009) was produced and purified as previously described (58), copper-saturated in the same way as *Sc*AA10C, and stored in the same buffer. Manganese-dependent SOD (MnSOD) from *Escherichia coli* (Sigma-Aldrich, S5639) was solubilized in Tris·HCl (10 mM, pH 8.0) and desalted (PD MidiTrap G-25, GE Healthcare) in the same buffer before use. HRP (type II) (Sigma-Aldrich, P8250) was solubilized in Milli-Q water and filtered (Filtropur S, 0.2 μm polyethersulfone (PES), Sarstedt). All enzymes were stored at 4 °C.

Standard Photobiocatalytic LPMO Reactions. Standard photobiocatalytic reactions were carried out in a cylindrical glass vial (1.1 mL) with a conical bottom (Thermo Fisher Scientific) with 500-μL reaction volume unless otherwise specified. The light source (Lightningcure L9588, Hamamatsu) was equipped with a filter with a spectral distribution of 400 to 700 nm (L9588-03, Hamamatsu) and placed ∼1 cm above the liquid surface. Typical reactions contained *Sc*AA10C (0.5 μM), Avicel (10 $g.L^{-1}$), and PE (5 $g.L^{-1}$) in sodium phosphate buffer (50 mM, pH 6.0). Reactions were incubated in the dark for 15 min at 40 °C under magnetic stirring before turning on the light (I = 10% I_{max}, equivalent to 16.8 $W.cm^{-2}$) or adding reductant (gallic acid), unless stated otherwise. To stop the LPMO reactions, 60-μL samples were taken from the reaction mixture at regular intervals and filtered using a 96-well filter plate (Millipore) and a vacuum manifold. Filtered samples (35 μL) were stored at −20 °C. Before quantifying the product by high-performance anion-exchange chromatography/pulsed amperometric detection (HPAEC-PAD) analysis, as described in the section *Product Analysis*, the filtrate was mixed with 35 μL of a 2-μM solution of purified Cel6A from *Themobifida fusca* (*Tf*Cel6A) (59), prepared in sodium phosphate buffer (50 mM, pH 6.0), and incubated at 40 °C overnight to convert solubilized oxidized cello-oligosaccharides to a mixture of C1-oxidized products with degrees of polymerization of 2 (GlcGlc1A) and 3 (Glc_2Glc1A). Reactions involving HRP were performed with nonwashed PE since nonwashed PE contains HRP substrates, which alleviates the need for adding the standard AmplexRed substrate. Reactions with SOD were performed using a 400-μL reaction volume instead of 500 μL.

Chitin Depolymerization Experiments. Chitin depolymerization reactions were performed with *Sm*AA10A (0.5 μM) in sodium phosphate buffer (50 mM, pH 6.0) with washed PE (10 $g.L^{-1}$). Reactions were stopped by filtration to separate soluble from insoluble products using a 96-well filter plate operated with a vacuum manifold (Merck Millipore). Before analysis using a Rezex column, 20 μL of sample was mixed with 20 μL of a 1-μM solution of purified chitobiase (*Sm*CHB) (42) and incubated overnight at room temperature to convert oxidized chito-oligosaccharides to GlcNAc and chitobionic acid, which were analyzed as described in the section *Product Analysis*.

Product Analysis. Oxidized cello-oligosaccharides were analyzed by HPAEC-PAD performed with a Dionex ICS5000 system (Dionex, Sunnyvale, CA) equipped with a CarboPac PA200 analytical column (3 × 250 mm) as previously described (60). Chromatograms were recorded and analyzed using Chromeleon 7.0 software. Quantitative analysis of C1-oxidizing LPMO activity was based on quantification of cellobionic acid (GlcGlc1A) and cellotrionic acid (Glc_2Glc1A), which were obtained after treating reaction filtrates with *Tf*Cel6A, as described in the section *Standard Photobiocatalytic LPMO Reactions*. Standards of GlcGlc1A and Glc_2Glc1A were prepared by treating cellobiose and cellotriose with cellobiose dehydrogenase (61).

Native and oxidized chito-oligosaccharides were analyzed by using a Dionex Ultimate 3000 High Performance Liquid Chromatography system (Dionex, Sunnyvale, CA), equipped with a Rezex RFQ-Fast Acid H+ (8%) 7.8 × 100 mm column (Phenomenex, Torrance, CA) preheated to 85 °C using 5 mM H_2SO_4 as mobile phase at a flow rate of 1 mL/min (62). The solutes were separated isocratically and were detected by using UV absorption at 194 nm. Solubilized GlcNAc and chitobionic acid were quantified based on standard curves for GlcNAc and chitobionic acid.

Total Reducing Capacity. The total reducing capacity of PE before and after washing was determined according to a published protocol that used gallic acid as a standard (32). This method is based on electron transfer from phenolic compounds to phosphomolybdic-phosphotungstic acid complexes in alkaline medium which can be spectrophotometrically measured. Non-washed and washed PE were suspended directly or after the last centrifugation step, respectively, in 95% (vol/vol) MeOH in concentrations ranging from 1.25 to 20 $g.L^{-1}$ in triplicates. Then 100-μL portions of the PE suspensions were transferred to 1.5-mL Eppendorf tubes to which 200 μL of a 10% (vol/vol) Folin-Ciocalteu reagent was added, followed by thorough mixing, addition of 800 μL Na_2CO_3 (0.7 M), thorough mixing, and a 2-h incubation at room temperature. The tubes were spun down for 1 min at 15,000 × *g* to remove any particles, and 200 μL of the resulting supernatant was transferred to 96-well microtiter plate also containing identically treated gallic acid samples to provide the standard curve (0 to 2,500 μM). The solutions were shaken for 10 s before recording the absorbance at 765 nm using a Varioskan Lux plate reader (Thermo Fisher Scientific).

H_2O_2 Accumulation. This method was adapted from previously published protocols (24, 40, 57). Reactions were performed in sodium phosphate buffer (50 mM; pH 6.0) with a total volume of 500 μL. Samples (75 μL) were taken after various time intervals and filtered as described in the section *Standard Photobiocatalytic LPMO Reactions*. To quantify the amount of accumulated H_2O_2, 50 μL of the filtered and, if needed, diluted sample was mixed with 25 μL H_2O and 25 μL of a premix composed of HRP (0.4 μM) and AmplexRed (0.4 mM) in sodium phosphate buffer (0.4 M, pH 6.0). The H_2O_2 standard curve (0, 10, 20, 30, 40 μM [final concentrations]) was prepared by mixing 25 μL of the same AmplexRed/HRP premix with 50 μL of the supernatant from a PE suspension with the same initial PE concentration as the reactions being measured (or appropriate dilutions thereof) to achieve approximately the same concentration of PE-derived components in the standard curve as in the reactions being measured, and lastly with 25 μL H_2O_2 solution (0, 40, 80, 120, 160 μM) in a 96-well microtiter plate. The reaction mixtures were shaken and incubated for 60 s at 30 °C before recording absorbance at 563 nm using a Varioskan Lux plate reader (Thermo Fisher Scientific).

Verification of SOD activity. SOD activity was assessed by using a published assay protocol (24, 63). In alkaline conditions, autooxidation of pyrogallol results in formation of a semiquinone and $O_2^{\bullet-}$, and the semiquinones further react to form purpurogallin, which absorbs strongly at 325 nm (63). Briefly, a stock solution of pyrogallol (2 mM) was prepared in 10 mM HCl, and stock solutions of SOD (0, 56.5, 113, 282.5, 565, 1,130, 2,825, and 5,650 nM) were prepared in Tris·HCl (10 mM, pH 8.0). Then 80 μL Tris·HCl (50 mM final reaction concentration, pH 8.0) was mixed with 10 μL SOD and 10 μL pyrogallol (0.2 mM final concentration) in a 96-well plate. The 96-well plate was shaken at 600 rpm for 5 s before recording absorbance at 325 nm every 8 s for 10 min using a Varioskan Lux plate reader (Thermo Fisher Scientific). The inhibitory effect of SOD on purpurogallin formation is shown in *SI Appendix*, Fig. S6.

Data, Materials, and Software Availability. All study data are included in the article and/or *SI Appendix*.

ACKNOWLEDGMENTS. We thank Ole Golten for providing the chitobiase (*Sm*CHB) and Susanne Zibek for helpful discussions. This work was supported by Norwegian Research Council Grant 262853 (E.G.K., F.S., and V.G.H.E.) and by the ChitoTex project funded by the German Federal Ministry of Education and Research through Grant 031A567A (T.H.).

Author affiliations: [a]Faculty of Chemistry, Biotechnology and Food Science, Norwegian University of Life Sciences (NMBU), 1432 Ås, Norway; and [b]Group Bioprocess Engineering, Fraunhofer Institute of Interfacial Engineering and Biotechnology, 70569 Stuttgart, Germany

1. X. Chen, S. Song, H. Li, G. Gözaydın, N. Yan, Expanding the boundary of biorefinery: Organonitrogen chemicals from biomass. *Acc. Chem. Res.* **54**, 1711–1722 (2021).
2. P. V. Harris *et al.*, Stimulation of lignocellulosic biomass hydrolysis by proteins of glycoside hydrolase family 61: Structure and function of a large, enigmatic family. *Biochemistry* **49**, 3305–3316 (2010).
3. G. Vaaje-Kolstad, S. J. Horn, D. M. F. van Aalten, B. Synstad, V. G. H. Eijsink, The non-catalytic chitin-binding protein CBP21 from *Serratia marcescens* is essential for chitin degradation. *J. Biol. Chem.* **280**, 28492–28497 (2005).
4. G. Vaaje-Kolstad *et al.*, An oxidative enzyme boosting the enzymatic conversion of recalcitrant polysaccharides. *Science* **330**, 219–222 (2010).
5. R. J. Quinlan *et al.*, Insights into the oxidative degradation of cellulose by a copper metalloenzyme that exploits biomass components. *Proc. Natl. Acad. Sci. U.S.A.* **108**, 15079–15084 (2011).
6. C. M. Phillips, W. T. Beeson, J. H. Cate, M. A. Marletta, Cellobiose dehydrogenase and a copper-dependent polysaccharide monooxygenase potentiate cellulose degradation by *Neurospora crassa*. *ACS Chem. Biol.* **6**, 1399–1406 (2011).
7. Z. Forsberg *et al.*, Cleavage of cellulose by a CBM33 protein. *Protein Sci.* **20**, 1479–1483 (2011).
8. A. Levasseur, E. Drula, V. Lombard, P. M. Coutinho, B. Henrissat, Expansion of the enzymatic repertoire of the CAZy database to integrate auxiliary redox enzymes. *Biotechnol. Biofuels* **6**, 41 (2013).
9. B. Bissaro *et al.*, Oxidative cleavage of polysaccharides by monocopper enzymes depends on H_2O_2. *Nat. Chem. Biol.* **13**, 1123–1128 (2017).
10. B. Bissaro *et al.*, Molecular mechanism of the chitinolytic peroxygenase reaction. *Proc. Natl. Acad. Sci. U.S.A.* **117**, 1504–1513 (2020).
11. J. A. Hangasky, A. T. Iavarone, M. A. Marletta, Reactivity of O_2 versus H_2O_2 with polysaccharide monooxygenases. *Proc. Natl. Acad. Sci. U.S.A.* **115**, 4915–4920 (2018).
12. S. M. Jones, W. J. Transue, K. K. Meier, B. Kelemen, E. I. Solomon, Kinetic analysis of amino acid radicals formed in H_2O_2-driven Cu^I LPMO reoxidation implicates dominant homolytic reactivity. *Proc. Natl. Acad. Sci. U.S.A.* **117**, 11916–11922 (2020).
13. T. M. Hedison *et al.*, Insights into the H_2O_2 -driven catalytic mechanism of fungal lytic polysaccharide monooxygenases. *FEBS J.* **288**, 4115–4128 (2021).
14. S. Kuusk *et al.*, Kinetic insights into the role of the reductant in H_2O_2-driven degradation of chitin by a bacterial lytic polysaccharide monooxygenase. *J. Biol. Chem.* **294**, 1516–1528 (2019).
15. S. Kuusk *et al.*, Kinetics of H_2O_2-driven degradation of chitin by a bacterial lytic polysaccharide monooxygenase. *J. Biol. Chem.* **293**, 523–531 (2018).
16. L. Rieder, D. Petrović, P. Väljamäe, V. G. H. Eijsink, M. Sørlie, Kinetic characterization of a putatively chitin-active LPMO reveals a preference for soluble substrates and absence of monooxygenase activity. *ACS Catal.* **11**, 11685–11695 (2021).
17. A. A. Stepnov *et al.*, The impact of reductants on the catalytic efficiency of a lytic polysaccharide monooxygenase and the special role of dehydroascorbic acid. *FEBS Lett.* **596**, 53–70 (2022).
18. K.-E. Eriksson, B. Pettersson, U. Westermark, Oxidation: An important enzyme reaction in fungal degradation of cellulose. *FEBS Lett.* **49**, 282–285 (1974).
19. B. Bissaro, A. Varnai, Å. K. Røhr, V. G. H. Eijsink, Oxidoreductases and reactive oxygen species in lignocellulose biomass conversion. *Microbiol. Mol. Biol. Rev.* **4**, e00029-18 (2018).
20. P. Chylenski *et al.*, Lytic polysaccharide monooxygenases in enzymatic processing of lignocellulosic biomass. *ACS Catal.* **9**, 4970–4991 (2019).
21. S. Kuusk, P. Väljamäe, Kinetics of H_2O_2-driven catalysis by a lytic polysaccharide monooxygenase from the fungus *Trichoderma reesei*. *J. Biol. Chem.* **297**, 101256 (2021).
22. L. H. Yang, C. Gratton, Insects as drivers of ecosystem processes. *Curr. Opin. Insect Sci.* **2**, 26–32 (2014).
23. M. M. C. H. van Schie *et al.*, Cascading g-C_3N_4 and peroxygenases for selective oxyfunctionalization reactions. *ACS Catal.* **9**, 7409–7417 (2019).
24. B. Bissaro, E. Kommedal, Å. K. Røhr, V. G. H. Eijsink, Controlled depolymerization of cellulose by light-driven lytic polysaccharide oxygenases. *Nat. Commun.* **11**, 890 (2020).
25. L. Schmermund *et al.*, Photo-biocatalysis: Biotransformations in the presence of light. *ACS Catal.* **9**, 4115–4144 (2019).
26. J. Kim, F. Hollmann, C. B. Park, Lignin as a multifunctional photocatalyst for solar-powered biocatalytic oxyfunctionalization of C-H bonds. *ChemRxiv* **1**, 217–226 (2021).
27. D. Cannella *et al.*, Light-driven oxidation of polysaccharides by photosynthetic pigments and a metalloenzyme. *Nat. Commun.* **7**, 11134 (2016).
28. B. Bissaro *et al.*, Fueling biomass-degrading oxidative enzymes by light-driven water oxidation. *Green Chem.* **18**, 5357–5366 (2016).
29. K. Y. Zhu, H. Merzendorfer, W. Zhang, J. Zhang, S. Muthukrishnan, Biosynthesis, turnover, and functions of chitin in insects. *Annu. Rev. Entomol.* **61**, 177–196 (2016).
30. S. O. Andersen, Insect cuticular sclerotization: A review. *Insect Biochem. Mol. Biol.* **40**, 166–178 (2010).
31. T. Hahn *et al.*, Purification of chitin from pupal exuviae of the black soldier fly. *Waste Biomass Valoriz.* **13**, 1993–2008 (2021).
32. E. A. Ainsworth, K. M. Gillespie, Estimation of total phenolic content and other oxidation substrates in plant tissues using Folin-Ciocalteu reagent. *Nat. Protoc.* **2**, 875–877 (2007).
33. S. O. Andersen, "Cuticular sclerotization and tanning" in *Insect Molecular Biology and Biochemistry*, L. I. Gilbert, Ed. (Academic Press, 2012), pp. 167–192.
34. G. Renger, T. Renger, Photosystem II: The machinery of photosynthetic water splitting. *Photosynth. Res.* **98**, 53–80 (2008).
35. P. Boule, A. Rossi, J. F. Pilichowski, G. Grabner, Photoreactivity of hydroquinone in aqueous-solution. *New J. Chem.* **16**, 1053–1062 (1992).
36. S. M. Beck, L. E. Brus, Photooxidation of water by *p*-benzoquinone. *J. Am. Chem. Soc.* **104**, 1103–1104 (1982).
37. K. C. Kurien, P. A. Robins, Photolysis of aqueous solutions of p-benzoquinone: A spectrophotometric investigation. *J. Chem. Soc. B Phys. Org.*, 855–859 (1970).
38. B. M. Blossom *et al.*, Photobiocatalysis by a lytic polysaccharide monooxygenase using intermittent illumination. *ACS Sustain. Chem.& Eng.* **8**, 9301–9310 (2020).
39. R. Xu *et al.*, Characterization of products from the reactions of N-acetyldopamine quinone with N-acetylhistidine. *Arch. Biochem. Biophys.* **329**, 56–64 (1996).
40. R. Kittl, D. Kracher, D. Burgstaller, D. Haltrich, R. Ludwig, Production of four *Neurospora crassa* lytic polysaccharide monooxygenases in *Pichia pastoris* monitored by a fluorimetric assay. *Biotechnol. Biofuels* **5**, 79 (2012).
41. Y. Pan *et al.*, Selective conversion of lignin model veratryl alcohol by photosynthetic pigment via photo-generated reactive oxygen species. *Chem. Eng. J.* **393**, 124772 (2020).
42. J. S. M. Loose, Z. Forsberg, M. W. Fraaije, V. G. H. Eijsink, G. Vaaje-Kolstad, A rapid quantitative activity assay shows that the *Vibrio cholerae* colonization factor GbpA is an active lytic polysaccharide monooxygenase. *FEBS Lett.* **588**, 3435–3440 (2014).
43. A. T. Austin, M. S. Méndez, C. L. Ballaré, Photodegradation alleviates the lignin bottleneck for carbon turnover in terrestrial ecosystems. *Proc. Natl. Acad. Sci. U.S.A.* **113**, 4392–4397 (2016).
44. A. T. Austin, L. Vivanco, Plant litter decomposition in a semi-arid ecosystem controlled by photodegradation. *Nature* **442**, 555–558 (2006).
45. A. T. Austin, C. L. Ballaré, Dual role of lignin in plant litter decomposition in terrestrial ecosystems. *Proc. Natl. Acad. Sci. U.S.A.* **107**, 4618–4622 (2010).
46. P. Berenstecher, L. Vivanco, L. I. Pérez, C. L. Ballaré, A. T. Austin, Sunlight doubles aboveground carbon loss in a seasonally dry woodland in Patagonia. *Curr. Biol.* **30**, 3243–3251.e3 (2020).
47. D. Kracher *et al.*, Extracellular electron transfer systems fuel cellulose oxidative degradation. *Science* **352**, 1098–1101 (2016).
48. R. Kont, B. Bissaro, V. G. H. Eijsink, P. Väljamäe, Kinetic insights into the peroxygenase activity of cellulose-active lytic polysaccharide monooxygenases (LPMOs). *Nat. Commun.* **11**, 5786 (2020).
49. R. M. Cory, G. W. Kling, Interactions between sunlight and microorganisms influence dissolved organic matter degradation along the aquatic continuum. *Limnol. Oceanogr. Lett.* **3**, 102–116 (2018).
50. R. Wolf, J.-E. Thrane, D. O. Hessen, T. Andersen, Modelling ROS formation in boreal lakes from interactions between dissolved organic matter and absorbed solar photon flux. *Water Res.* **132**, 331–339 (2018).
51. Y. Bai, V. G. H. Eijsink, A. M. Kielak, J. A. van Veen, W. de Boer, Genomic comparison of chitinolytic enzyme systems from terrestrial and aquatic bacteria. *Environ. Microbiol.* **18**, 38–49 (2016).
52. E. Miglbauer, M. Gryszel, E. D. Głowacki, Photochemical evolution of hydrogen peroxide on lignins. *Green Chem.* **22**, 673–677 (2020).
53. A. J. Ragauskas *et al.*, Lignin valorization: Improving lignin processing in the biorefinery. *Science* **344**, 1246843 (2014).
54. H. E. Bonfield *et al.*, Photons as a 21st century reagent. *Nat. Commun.* **11**, 804 (2020).
55. A. Kadić, A. Várnai, V. G. H. Eijsink, S. J. Horn, G. Lidén, In situ measurements of oxidation-reduction potential and hydrogen peroxide concentration as tools for revealing LPMO inactivation during enzymatic saccharification of cellulose. *Biotechnol. Biofuels* **14**, 46 (2021).
56. F. Sabbadin *et al.*, Secreted pectin monooxygenases drive plant infection by pathogenic oomycetes. *Science* **373**, 774–779 (2021).
57. A. A. Stepnov *et al.*, Unraveling the roles of the reductant and free copper ions in LPMO kinetics. *Biotechnol. Biofuels* **14**, 28 (2021).
58. G. Vaaje-Kolstad, D. R. Houston, A. H. K. Riemen, V. G. H. Eijsink, D. M. F. van Aalten, Crystal structure and binding properties of the *Serratia marcescens* chitin-binding protein CBP21. *J. Biol. Chem.* **280**, 11313–11319 (2005).
59. R. E. Calza, D. C. Irwin, D. B. Wilson, Purification and characterization of two β-1,4-endoglucanases from *Thermomonospora fusca*. *Biochemistry* **24**, 7797–7804 (1985).
60. B. Westereng *et al.*, Efficient separation of oxidized cello-oligosaccharides generated by cellulose degrading lytic polysaccharide monooxygenases. *J. Chromatogr. A* **1271**, 144–152 (2013).
61. M. Zámocký *et al.*, Cloning, sequence analysis and heterologous expression in *Pichia pastoris* of a gene encoding a thermostable cellobiose dehydrogenase from *Myriococcum thermophilum*. *Protein Expr. Purif.* **59**, 258–265 (2008).
62. S. Mekasha *et al.*, A trimodular bacterial enzyme combining hydrolytic activity with oxidative glycosidic bond cleavage efficiently degrades chitin. *J. Biol. Chem.* **295**, 9134–9146 (2020).
63. X. Li, Improved pyrogallol autoxidation method: A reliable and cheap superoxide-scavenging assay suitable for all antioxidants. *J. Agric. Food Chem.* **60**, 6418–6424 (2012).